

# The minimal $B - L$ model naturally realized at TeV scale

Satoshi Iso<sup>a,1</sup>, Nobuchika Okada<sup>a,b,2</sup> and Yuta Orikasa<sup>a,3</sup>

<sup>a</sup> *KEK Theory Center,*

*High Energy Accelerator Research Organization (KEK)*

*and*

*Department of Particles and Nuclear Physics,*

*The Graduate University for Advanced Studies (SOKENDAI),*

*1-1 Oho, Tsukuba, Ibaraki 305-0801, Japan*

<sup>b</sup> *Department of Physics and Astronomy,*

*University of Alabama,*

*Tuscaloosa, AL 35487, USA*

## Abstract

In a previous paper [1], we have proposed the minimal  $B - L$  extended standard model as a phenomenologically viable model that realizes the Coleman-Weinberg-type breaking of the electroweak symmetry. Assuming the classical conformal invariance and stability up to the Planck scale, we will show in this paper that the model naturally predicts TeV scale  $B - L$  breaking as well as a light standard-model singlet Higgs boson and light right-handed neutrinos around the same energy scale. We also study phenomenology and detectability of the model at the Large Hadron Collider (LHC) and the International Linear Collider (ILC).

---

<sup>1</sup>satoshi.iso@kek.jp

<sup>2</sup>okadan@post.kek.jp

<sup>3</sup>orikasa@post.kek.jp

# 1 Introduction

To understand the dynamics of the electroweak symmetry breaking is one of the most important issues in particle physics. In particular, the hierarchy problem, i.e. the stability of the electroweak scale against a higher energy scale (e.g. GUT scale or Planck scale) is the most mysterious. Low energy supersymmetry provides a natural solution, and predicts new particles around the TeV scale. It also predicts a relatively light Higgs boson mass below 130 GeV compared to the standard model (SM) theoretical bound  $130 \text{ GeV} \lesssim m_h \lesssim 170 \text{ GeV}$  imposed by the triviality and the stability of the electroweak vacuum.

We should, however, also be prepared for a case of a heavier Higgs boson and no signals of supersymmetry at the experiment. In this case, there may be various possibilities, but here we pay a special attention to the (almost) classical conformal invariance of the SM. Because of the chiral nature, the SM Lagrangian at the classical level cannot possess dimensionful parameters except for the Higgs mass term closely related to the gauge hierarchy problem.

A common wisdom is that, even if the SM Lagrangian possesses the classical conformal invariance, the Higgs mass term is radiatively induced by matter fields with quadratically divergent coefficients, and hence we cannot be free from the gauge hierarchy problem. Bardeen has argued [2] that once the classical conformal invariance and its minimal violation by quantum anomalies are imposed on the SM, it may be free from the quadratic divergences and hence the gauge hierarchy problem. It seems difficult to realize such a mechanism in ordinary field theories based on the Wilsonian renormalization group, but we cannot either deny a possibility of an yet unknown mechanism to forbid the quadratic (and possibly the quartic) divergences in field theories based on the Planck scale physics (see e.g. [3]). Such a mechanism inevitably requires the absence of intermediate mass scales between the electroweak and the Planck scales. In other words, physics at the Planck scale is directly connected with the electroweak physics.

In this paper, we do not further discuss the mechanism itself, but investigate its phenomenological implications. If the quadratic divergences are absent in classically conformal theories, the conformal symmetry is broken only by the logarithmic running of the coupling constants. As a result, the electroweak symmetry breaking is realized not by the negative mass squared term of the Higgs doublet, but the radiative breaking a la Coleman-Weinberg (CW) [4]. It is, however, well-recognized that the CW scenario is already excluded for the SM because of the large top-Yukawa coupling. In the original paper [4] by Coleman and Weinberg, they predicted the Higgs boson mass at 10 GeV assuming a small top-quark mass, but at present, the heavy top-quark is known to destabilize the Higgs potential, and the CW mechanism does not work (see, e.g., [1]). Hence we should extend the SM so that the CW mechanism works with phenomenologically viable parameters. Along this philosophy, Meissner and Nicolai [5] investigated

extensions of the SM with the classical conformal invariance (see also earlier works [6, 7, 8, 9]).

In a previous paper [1], inspired by the work [5], we have proposed a minimal phenomenologically viable model that the electroweak symmetry can be radiatively broken. It is the minimal  $B - L$  model [10, 11], i.e. a  $B - L$  (baryon number minus lepton number) gauged extension of the SM with the right-handed neutrinos and a SM singlet scalar field ( $\Phi$ ) with two units of  $B - L$  charge. The model is similar to the one proposed by Meissner and Nicolai [5], but the difference is whether the  $B - L$  symmetry is gauged or not. In [1] we showed that the gauging of  $B - L$  symmetry plays the important role to achieve the radiative  $B - L$  symmetry breaking. Without gauging, the Renormalization Group (RG) improved effective potential of  $\Phi$  does not have a minimum (see discussions after Eq. (13)). It is also phenomenologically favorable.

Such a model is strongly constrained by the following theoretical requirements:

- Classical conformal invariance
- Stability of the Higgs potential up to the Planck scale
- No other intermediate mass scales

The electroweak as well as the  $B - L$  symmetries should be broken radiatively by the CW mechanism because of the classical conformal invariance. The condition that the theory is stable up to the Planck scale gives a strong constraint on the parameter space of the model. The stability of the electroweak scale against radiative corrections gives upper bounds for the masses of the  $B - L$  gauge boson and the right-handed neutrinos, and in this way we are led to the minimal  $B - L$  gauged model *naturally realized at the TeV scale*.

In this paper, we further study the theoretical and phenomenological properties of the model. We first summarize the predictions of our model. In addition to the SM particles, the model consists of the following new particles:

- gauge boson  $Z'$  associated with the  $B - L$  gauge symmetry
- right-handed neutrinos  $\nu_R^i$
- SM singlet Higgs  $\Phi$  which breaks the  $B - L$  gauge symmetry and gives the right-handed neutrinos masses

Because of the theoretical requirements, we have various predictions for these particles. The most important prediction is drawn in Fig. 5. The figure shows an allowed region of the  $Z'$  boson mass ( $m_{Z'}$ ) and the  $B - L$  gauge coupling ( $\alpha_{B-L}$ ). If the value of the  $B - L$  gauge

coupling is around the same order as those of the SM gauge couplings ( $\alpha_{B-L} \sim 0.01$ ),  $Z'$  gauge boson mass is predicted to be around a few TeV,

$$m_{Z'} \sim \text{a few TeV} \quad (1)$$

and will be soon discovered at the LHC.

Another important prediction is drawn in Fig. 2. The figure shows a ratio of  $m_\phi$  and  $m_{Z'}$  as a function of the Yukawa coupling of the right-handed neutrino divided by  $\alpha_{B-L}$ . The scalar mass  $m_\phi$  is much smaller than the  $Z'$  mass. This is a general consequence of the CW type symmetry breaking where the potential minimal is realized by the balance between the tree level quartic Higgs potential and the 1-loop potential. If the Yukawa couplings of the right-handed neutrinos are negligible, there is a simple relation for the mass ratio,

$$\left(\frac{m_\phi}{m_{Z'}}\right)^2 \simeq \frac{6}{\pi} \alpha_{B-L} \ll 1. \quad (2)$$

If the Yukawa couplings of the right-handed neutrinos are larger, the scalar mass  $m_\phi$  becomes much smaller. The figure is drawn for the largest possible value of  $\alpha_{B-L} \sim 0.01$ . The mass ratio becomes smaller for a smaller value of  $\alpha_{B-L}$  or with the effect of the right-handed neutrino Yukawa coupling. Hence  $m_\phi$  is always lighter than  $0.14 m_{Z'}$ .

The figure also shows that, when the Majorana mass of the right-handed neutrino becomes larger than a critical value, it destabilizes the vacuum. Hence our model gives an upper bound for the Majorana mass of the right-handed neutrinos  $m_N^2 \lesssim 2.5 m_{Z'}^2$ . At the maximum value of  $m_N$ , the SM singlet Higgs boson  $\phi$  becomes almost massless. Hence the right-handed neutrinos are expected to be similar to or lighter than  $Z'$  gauge boson. The lightness of the right-handed neutrinos is another prediction of the model.

The paper is organized as follows. In section 2, we first introduce our model and review the analysis of the symmetry breaking studied in the previous paper. In section 3, we discuss the theoretical constraints on the masses of the new particles. In section 4, we study the phenomenology of the model. Since all the new particles should be around the TeV scale, a rich phenomenology can be expected at future collider experiments. We first study the physics of the  $Z'$  gauge boson, which can be easily detected. Once  $Z'$  gauge boson is found, it is a portal to the  $B-L$  breaking sector and to the right-handed neutrino sector. The singlet Higgs boson can be produced associated with the  $Z'$  boson in the same manner as the SM Higgs boson production associated with the  $Z$  boson. If kinematically allowed,  $Z'$  boson can decay into a pair of right-handed neutrinos and the nature of the seesaw mechanism can be revealed through this decay mode.

	$SU(3)_c$	$SU(2)_L$	$U(1)_Y$	$U(1)_{B-L}$
$q_L^i$	<b>3</b>	<b>2</b>	+1/6	+1/3
$u_R^i$	<b>3</b>	<b>1</b>	+2/3	+1/3
$d_R^i$	<b>3</b>	<b>1</b>	-1/3	+1/3
$\ell_L^i$	<b>1</b>	<b>2</b>	-1/2	-1
$\nu_R^i$	<b>1</b>	<b>1</b>	0	-1
$e_R^i$	<b>1</b>	<b>1</b>	-1	-1
$H$	<b>1</b>	<b>2</b>	-1/2	0
$\Phi$	<b>1</b>	<b>1</b>	0	+2

Table 1: Particle contents. In addition to the SM particle contents, the right-handed neutrino  $\nu_R^i$  ( $i = 1, 2, 3$  denotes the generation index) and a complex scalar  $\Phi$  are introduced.

## 2 Radiative symmetry breakings

### 2.1 Classically conformal $B - L$ model

We first review our model. It is the minimal  $B - L$  extension of the SM [10] with the classical conformal symmetry, and based on the gauge group  $SU(3)_c \times SU(2)_L \times U(1)_Y \times U(1)_{B-L}$ . The particle contents (except for the gauge bosons) are listed in Table 1 [11]. Here, three generations of right-handed neutrinos ( $\nu_R^i$ ) are necessarily introduced to make the model free from all the gauge and gravitational anomalies. The SM singlet scalar field ( $\Phi$ ) works to break the  $U(1)_{B-L}$  gauge symmetry by its VEV and at the same time, generates the right-handed neutrino masses.

The Lagrangian relevant for the seesaw mechanism is given as

$$\mathcal{L} \supset -Y_D^{ij} \overline{\nu_R^i} H^\dagger \ell_L^j - \frac{1}{2} Y_N^i \Phi \overline{\nu_R^i} \nu_R^i + \text{h.c.}, \quad (3)$$

where the first term gives the Dirac neutrino mass term after the electroweak symmetry breaking, while the right-handed neutrino Majorana mass term is generated through the second term associated with the  $B - L$  gauge symmetry breaking. Without loss of generality, we here work on the basis where the second term is diagonalized and  $Y_N^i$  is real and positive.

Under the hypothesis of the classical conformal invariance of the model, the classical scalar potential is described as

$$V = \lambda_H (H^\dagger H)^2 + \lambda (\Phi^\dagger \Phi)^2 + \lambda' (\Phi^\dagger \Phi) (H^\dagger H). \quad (4)$$

Note that when  $\lambda'$  is negligibly small, the SM Higgs sector and the  $\Phi$  sector relevant for the  $B - L$  symmetry breaking are approximately decoupled. If this is the case, we can separately analyze these two Higgs sectors. When the Yukawa coupling  $Y_N$  is negligible compared to the

$U(1)_{B-L}$  gauge coupling, the  $\Phi$  sector is the same as the original Coleman-Weinberg model [4], so that the radiative  $U(1)_{B-L}$  symmetry breaking will be achieved. Once  $\Phi$  develops its VEV, the tree-level mass term for the SM Higgs doublet is effectively generated through the third term in Eq. (4). Taking  $\lambda'$  negative, the induced mass squared is negative and as a result, the electroweak symmetry breaking is driven in the same way as in the SM.

Because of the requirement of the classical conformal invariance, the model is characterized by a very few parameters, i.e. besides the SM couplings, the Dirac and Majorana Yukawa couplings for neutrinos, the model has only the following 4 additional parameters:

1.  $B - L$  gauge coupling ( $\alpha_{B-L}$ )
2. Higgs quartic coupling ( $\lambda_H$ )
3. SM singlet Higgs quartic coupling ( $\lambda$ )
4. Mixing between  $\Phi$  and  $H$  ( $\lambda'$ ).

These four parameters determine the  $B - L$  breaking scale  $M$ , the electroweak breaking scale  $v = 246$  GeV,  $m_{Z'}$ ,  $m_\phi$  and the Higgs boson mass  $m_H$ . There is a relation between  $M$ ,  $m_{Z'}$  and  $m_\phi$  because of the absence of the tree level mass term for the  $\Phi$  field.

## 2.2 $B - L$ Symmetry Breaking

Without the mass terms in the scalar potential, the symmetry breaking must occur radiatively. Generally speaking, we need to study the full effective potential for the two Higgs fields  $H$  and  $\Phi$  [12]. However, since the  $B - L$  breaking scale  $M$  must be phenomenologically higher than the electroweak scale  $v$  (at least one-order of magnitude), we can separately analyze the  $B - L$  and the electroweak symmetry breakings. In other words, since we should have a relation  $\langle \Phi \rangle \gg \langle H \rangle$ , we can first neglect the  $H$  field and calculate the Coleman-Weinberg potential along the  $\Phi$  direction. Then we can investigate the radiative breaking of the electroweak symmetry. The mixing term with a negative coupling,  $\lambda'(\Phi^\dagger\Phi)(H^\dagger H)$ , triggers the electroweak symmetry breaking. The validity of this approximation can be justified for the phenomenologically favorable parameters [1].

Let us first investigate the radiative  $B - L$  symmetry breaking. We renormalize the CW effective potential at the one-loop level as [13, 14]

$$V(\phi) = \frac{1}{4}\lambda(t)G^4(t)\phi^4, \quad (5)$$

where  $\phi/\sqrt{2} = \Re[\Phi]$ ,  $t = \log[\phi/M]$  with the renormalization point  $M$ , and

$$G(t) = \exp \left[ - \int_0^t dt' \gamma(t') \right]. \quad (6)$$

The anomalous dimension (in the Landau gauge) is given by

$$\gamma = \frac{1}{32\pi^2} \left[ \sum_i (Y_N^i)^2 - a_2 g_{B-L}^2 \right]. \quad (7)$$

Here,  $g_{B-L}$  is the  $B - L$  gauge coupling, and  $a_2 = 24$ . Renormalization group equations for coupling parameters involved in our analysis are listed below:

$$\begin{aligned} 2\pi \frac{d\alpha_{B-L}}{dt} &= b\alpha_{B-L}^2, \\ 2\pi \frac{d\alpha_\lambda}{dt} &= a_1\alpha_\lambda^2 + 8\pi\alpha_\lambda\gamma + a_3\alpha_{B-L}^2 - \frac{1}{2} \sum_i (\alpha_N^i)^2, \\ \pi \frac{d\alpha_N^i}{dt} &= \alpha_N^i \left( \frac{1}{2}\alpha_N^i + \frac{1}{4} \sum_j \alpha_N^j - 9\alpha_{B-L} \right), \end{aligned} \quad (8)$$

where  $\alpha_{B-L} = g_{B-L}^2/(4\pi)$ ,  $\alpha_\lambda = \lambda/(4\pi)$ ,  $\alpha_N^i = (Y_N^i)^2/(4\pi)$ , and the coefficients in the beta functions are explicitly given as  $b = 12$ ,  $a_1 = 10$  and  $a_3 = 48$ .

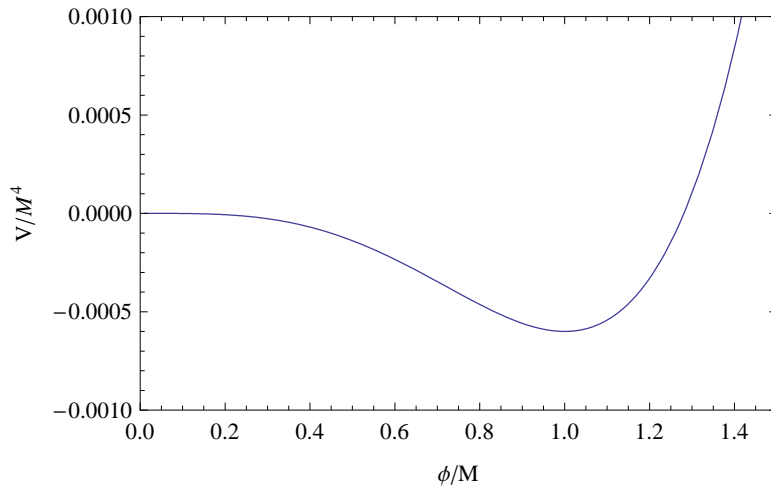


Figure 1: The RG improved effective potential. Here, we have taken  $\alpha_{B-L}(0) = 0.01$  and  $\alpha_N = 0$  for simplicity.

By solving the RG equations, we can obtain the RG improved effective potential. Please refer to [1] for more details of the solution. The Figure 1 depicts the RG-improved effective

potential<sup>1</sup> and it has a minimum at  $\phi = M$ .

The condition for the potential to have a minimum can be obtained without solving the RG equations. Setting the renormalization point to be the VEV of  $\phi$  at the potential minimum ( $\phi = M$  or equivalently  $t = 0$ ), the stationary condition  $\left. \frac{dV}{d\phi} \right|_{\phi=M} = 0$  leads to a relation among the coupling constants at the potential minimum (at  $t = 0$ )

$$\frac{d\alpha_\lambda}{dt} + 4\alpha_\lambda(1 - \gamma) = \frac{1}{2\pi} \left( 10\alpha_\lambda^2 + 48\alpha_{B-L}^2 - \frac{1}{2} \sum_i (\alpha_N^i)^2 \right) + 4\alpha_\lambda = 0. \quad (9)$$

For coupling values well within the perturbative regime,  $\alpha_\lambda \sim \alpha_{B-L}^2 \sim (\alpha_N^i)^2 \ll 1$ , we find the relation

$$\alpha_\lambda(0) \simeq -\frac{6}{\pi} \left( \alpha_{B-L}(0)^2 - \frac{1}{96} \sum_i (\alpha_N^i(0))^2 \right). \quad (10)$$

This is the dimensional transmutation, and one of the independent couplings is transmuted to the energy scale  $M$  of the  $B - L$  breaking.

The mass of the SM singlet Higgs  $\phi$  can be obtained by taking the second derivative of the effective potential at the minimum and given by

$$m_\phi^2 = \left. \frac{d^2V}{d\phi^2} \right|_{\phi=M} \simeq -16\pi\alpha_\lambda(0)M^2. \quad (11)$$

The coupling  $\alpha_\lambda(0)$  satisfies the relation Eq. (10). We should note here that the physical coupling constant at the minimum is given by taking the fourth derivatives of the potential as

$$\lambda_{eff} = \left. \frac{\partial^4 V}{\partial \phi^4} \right|_{t=0} = -\frac{22}{3}\lambda(0). \quad (12)$$

Then the SM singlet Higgs boson mass is given in terms of the physical (effective) coupling by

$$m_\phi^2 = \frac{24\pi}{11}\alpha_{\lambda,eff}M^2. \quad (13)$$

Therefore, the effective potential has a minimum at  $\phi = M$  and the  $B - L$  symmetry is radiatively broken, only the condition  $\alpha_\lambda(0) < 0$  is satisfied. In the limit  $\alpha_N^i \rightarrow 0$ , the system is the same as the one originally investigated by Coleman-Weinberg [4], where the U(1) gauge interaction plays the crucial role to achieve the radiative symmetry breaking keeping the validity of perturbation. In this sense, gauging the U(1)<sub>B-L</sub> is necessary although it is not required for the purpose to implement the seesaw mechanism.

---

<sup>1</sup>The RG improved effective potential has an infrared instability, but it is far below the QCD scale [1] and invisible in the figure. Since the perturbative calculation is not reliable there, the instability itself cannot be justifiably investigated. Hence we do not consider it here.



### 2.3 Electroweak symmetry breaking

Now let us consider the SM Higgs sector. In our model, the electroweak symmetry breaking is achieved in a very simple way. Once the  $B - L$  symmetry is broken, the SM Higgs doublet mass ( $\mu^2 h^2/2$ ) is generated through the mixing term between  $H$  and  $\Phi$  in the scalar potential (see Eqs. (4)),

$$\mu^2 = \frac{\lambda'}{2} M^2. \quad (14)$$

Choosing  $\lambda' < 0$ , the electroweak symmetry is broken in the same way as in the SM. However, the crucial difference from the SM is that in our model, the electroweak symmetry breaking originates from the radiative breaking of the  $U(1)_{B-L}$  gauge symmetry. At the tree level the Higgs boson mass is given by  $m_h^2 = 2|\mu^2| = |\lambda'|M^2 = 2\lambda_H v^2$  where  $\langle h \rangle = v = 246$  GeV. Then, by imposing the triviality (up to the Planck scale) and the vacuum stability bounds, the Higgs boson mass is given in a range  $130 \text{ GeV} \lesssim m_h \lesssim 170 \text{ GeV}$  as in the SM [15].

In the case of the ordinary Coleman-Weinberg scenario for the SM, the large top-Yukawa coupling causes the instability of the effective Higgs potential. In the present case, however, the introduction of the  $B - L$  sector saves this instability, and the Coleman-Weinberg mechanism can be dynamically realized. This is the theoretical reason why the  $B - L$  gauge sector is necessary to realize the Coleman-Weinberg mechanism.

## 3 Theoretical constraints on $m_{Z'}$ , $m_\phi$ and $m_N$

Due to the theoretical requirements discussed in the introduction, the parameter space of the model can be highly constrained. The classical conformal invariance reduces the number of the new coupling constants. Then the triviality and the stability of the Higgs potential up to the Planck scale strongly constrain values of the coupling constants. Furthermore naturalness of the electroweak scale against the mass scale in the  $B - L$  sector constrains the masses of  $Z'$  and the right-handed neutrinos to be lighter than a few TeV. In this section we discuss these theoretical constraints on  $m_{Z'}$ ,  $m_\phi$  and  $m_N$ .

### 3.1 Mass formula

One of the two parameters in the  $B - L$  sector ( $\alpha_{B-L}$ ,  $\lambda$ ) is used to determine the  $B - L$  symmetry breaking scale  $M$ . Hence a relation arises between the masses of  $Z'$  and  $\phi$ . This is due to the absence of the tree level mass term in the classical Lagrangian of  $\Phi$ . On the contrary, in the SM Higgs sector, the additional coupling  $|H|^2|\langle\Phi\rangle|^2$  gives the mass term of the Higgs

doublet  $H$ , and then the SM Higgs mass can be taken independently of the mass of the SM gauge bosons.

An extra gauge boson associated with the  $U(1)_{B-L}$  gauge symmetry acquires its mass through the  $B-L$  symmetry breaking. It is given by

$$m_{Z'}^2 = 16\pi\alpha_{B-L}(0)M^2. \quad (15)$$

The coupling constant  $\alpha_{B-L}$  is bounded from above by a condition that the running  $B-L$  coupling does not diverge up to the Planck scale. Roughly it is bounded as  $\alpha_{B-L}(0) < 0.015$ . The constraint is drawn in Fig. 5 as a almost straight line (in green).

On the other hand, the SM singlet Higgs mass is given by Eq. (13) and we can find the mass relation between  $Z'$  boson and the SM singlet Higgs boson

$$\left(\frac{m_\phi}{m_{Z'}}\right)^2 \simeq \frac{6}{\pi} \left( \alpha_{B-L} - \frac{1}{96} \frac{\sum_i (\alpha_N^i)^2}{\alpha_{B-L}} \right) \lesssim 0.03. \quad (16)$$

The maximum value of the mass ratio is given by the maximum  $\alpha_{B-L}$  and neglecting the Majorana coupling  $\alpha_N$ .

The hierarchy between the two masses is a general consequence of the Coleman-Weinberg model where the symmetry breaking occurs under the balance between the tree-level quartic coupling and the terms generated by quantum corrections. The scalar boson  $\phi$  can be much lighter than the  $Z'$  gauge boson and possibly comparable with the SM Higgs boson. Then, as we discuss later, the two scalars mix each other.

Eq. (16) indicates that as the Yukawa coupling  $\alpha_N$  becomes larger, the SM singlet Higgs boson mass squared is reducing and eventually changes its sign. Therefore, there is an upper limit on the Yukawa coupling in order for the effective potential to have the minimum at  $\phi = M$  ( $t = 0$ ). This is in fact the same reason as why the Coleman-Weinberg mechanism in the SM Higgs sector fails to break the electroweak symmetry when the top-Yukawa coupling is large as observed. Analyzing the RG improved effective potential with only one Yukawa coupling  $\alpha_N$ , the SM singlet Higgs boson mass as a function of the Yukawa coupling is depicted in Fig. 2. The minimum at  $M$  in the effective potential changes into the maximum for  $\alpha_N(0) > 9.8\alpha_{B-L}(0)$ .

The Majorana mass of the right-handed neutrinos must be lighter than the critical value discussed above;

$$m_N^2 = Y_N^2 M^2 = 4\pi\alpha_N M^2 < \sqrt{6}m_{Z'}^2. \quad (17)$$

At the maximum value of  $m_N$ , the SM singlet Higgs becomes almost massless. Hence the right-handed neutrinos are expected to be similar to or lighter than  $m_{Z'}$ . This is another important prediction of our model.

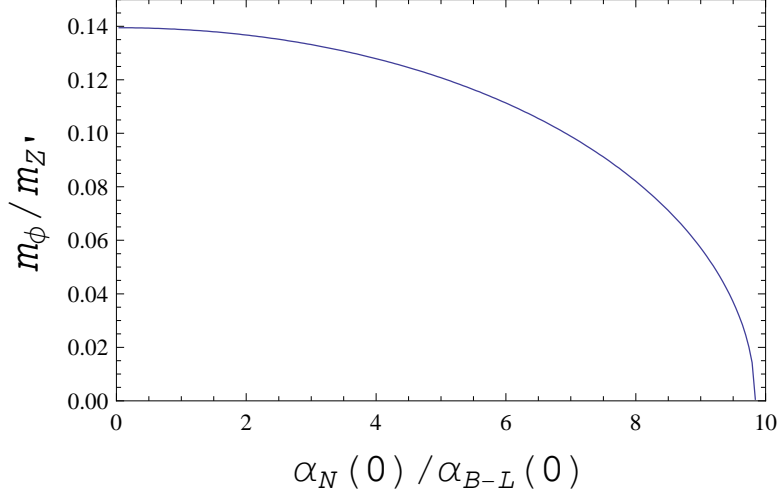


Figure 2: The SM singlet Higgs boson mass as a function of the Yukawa coupling. Here we have taken  $\alpha_{B-L}(0) = 0.01$  and accordingly, fixed  $\alpha_\lambda(0)$  to satisfy the stationary condition in Eq. (9). For  $\alpha_N(0) \simeq 9.8\alpha_{B-L}(0)$ , the potential minimum at  $\phi = M$  changes into the maximum.

### 3.2 Naturalness constraints on $m_{Z'}$ and $m_N$

We have imposed the classical conformal invariance and the absence of the quadratic divergences to solve the gauge hierarchy problem. This itself should be solved by the physics at the Planck scale, but we should also take care of the loop effects of heavy states in the theory associated with the  $B-L$  breaking, since there is a small hierarchy between the electroweak scale  $v = 246$  GeV and the  $B-L$  breaking scale  $M$ . Here we estimate the effects by the loop diagrams of heavy states on the Higgs boson mass carefully, and leads to upper bounds on masses of heavy states in terms of naturalness.

The states whose masses are associated with the  $B-L$  breaking scale are  $Z'$  gauge boson, SM singlet Higgs boson  $\phi$  and the right-handed neutrinos  $\nu_R^i$ . Since the coupling  $\lambda'$  between the SM singlet Higgs and the SM Higgs doublet is tiny, the stability of the electroweak scale does not give a strong constraint on the mass of  $\phi$ . Hence we will consider the effects of the right-handed neutrinos and the  $Z'$  gauge boson.

We first consider the one-loop effect of the right-handed neutrinos  $\nu_R^i$ . A typical graph with  $\nu_R$  contributing to the Higgs potential is given by Fig. 3. When the SM singlet gets the VEV  $\phi = M$ , we obtain the effective Higgs boson mass squared such as

$$\Delta m_h^2 \sim \frac{Y_D^2 Y_N^2}{16\pi^2} M^2 \log \frac{M_{Pl}^2}{m_{Z'}^2} \sim \frac{m_\nu m_N^3}{16\pi^2 v^2} \log \frac{M_{Pl}^2}{m_{Z'}^2}, \quad (18)$$

where we have used the seesaw formula,  $m_\nu \sim Y_D^2 v^2 / m_N$  with  $m_N = Y_N M$ . For the stability of the electroweak vacuum,  $\Delta m_h^2$  should be smaller than the electroweak scale. (The condition

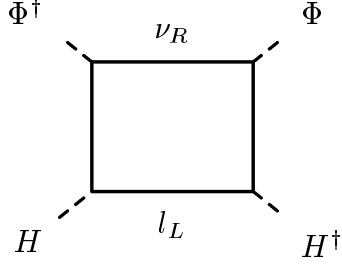


Figure 3: One-loop diagram inducing the mixing term  $(\Phi^\dagger\Phi)(H^\dagger H)$  through the right-handed neutrinos.

is equivalent to the *naturalness* of the  $\lambda'$  coupling.) Thus, we can obtain the upper bound of  $m_N$  once  $m_\nu$  is fixed. For example, when the neutrino mass is around  $m_\nu \sim 0.1$  eV, there is an upper bound for the Majorana mass  $m_N \lesssim 2.4 \times 10^6$  GeV and hence  $M \lesssim 2.4 \times 10^6/Y_N$  GeV. A similar constraint on the Majorana mass was found in [16]. In our model, the constraint is milder than Eq. (17) imposed by the stability of the potential.

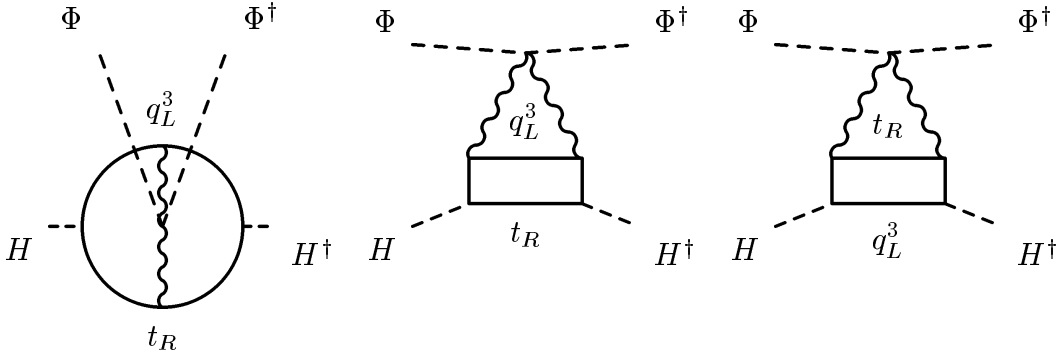


Figure 4: Two-loop diagrams inducing the mixing term  $(\Phi^\dagger\Phi)(H^\dagger H)$  through the top-quarks and the  $B - L$  gauge bosons. The wavy lines represent the propagators of the  $B - L$  gauge bosons.

The second, but more important constraint comes from two-loop effects (see Fig. 4) involving the top-quarks and the  $Z'$  gauge boson. Because of the large top-quark Yukawa coupling, these diagrams give significant contributions. The detail of the calculations is given in Appendix. By substituting  $\phi = M$  in the above diagrams, we obtain the correction such as

$$\Delta m_h^2 = \frac{8\alpha_{B-L} m_t^2 m_{Z'}^2}{(4\pi)^3} \log \frac{M_{Pl}^2}{m_{Z'}^2}. \quad (19)$$

Note that the  $(\log[M_{Pl}/m_{Z'}])^2$  term vanishes, and the Higgs mass correction depends linearly on the logarithm. In order to assure the naturalness of the Higgs boson mass, this correction

cannot be much larger than the electroweak scale. This gives a stringent constraint on the  $Z'$  mass, which is drawn in Fig. 5 as a solid curve (in red). The upper-right side of it is disfavored by the naturalness condition.

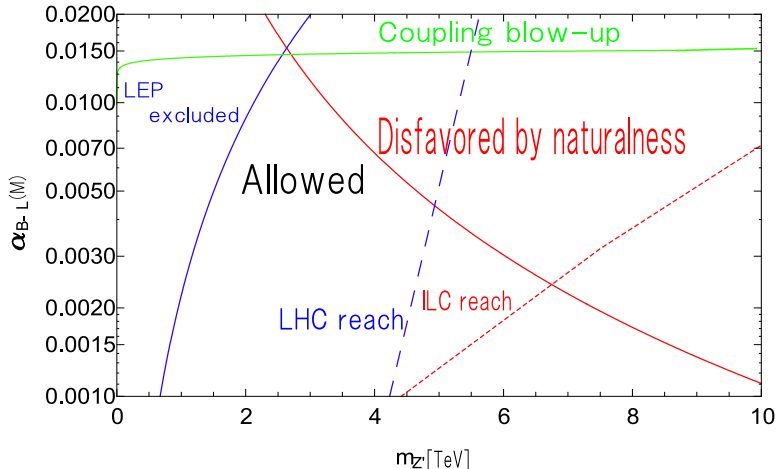


Figure 5: The allowed parameter region is drawn. The upper region of the almost straight line (in green) is rejected by a requirement that the  $B - L$  gauge coupling does not diverge up to the Planck scale. The upper-right side of the solid line (in red) is disfavored by the naturalness condition of the electroweak scale. The left of the solid line (in blue) has been already excluded by the LEP experiment,  $M \gtrsim 3$  TeV. The left of the dashed line can be explored in  $5\text{-}\sigma$  significance at the LHC with  $\sqrt{s}=14$  TeV and an integrated luminosity  $100 \text{ fb}^{-1}$ . The left of the dotted line can be explored at the ILC with  $\sqrt{s}=1$  TeV, assuming 1% accuracy.

In Fig. 5, the upper region of the straight line (in green) at  $\alpha_{B-L} \sim 0.015$  is rejected by a requirement that the  $B - L$  gauge coupling does not diverge up to the Planck scale. The upper-right side of the solid line (in red) is disfavored by the naturalness condition discussed above. The left of the solid line (in blue) has been already excluded by the LEP experiment,  $M \gtrsim 3$  TeV [17], which is consistent with the bound from the direct search for  $Z'$  boson at Tevatron [18]. The figure indicates that if the  $B - L$  gauge coupling is not much smaller than the SM gauge couplings, e.g.  $0.005 \lesssim \alpha_{B-L} \lesssim 0.015$ , the mass of the  $Z'$  gauge boson is constrained to be around a few TeV. The left of the dashed (dotted) lines can be reached at the LHC (ILC) experiment. We will discuss this search reach in the next section. Hence, most of the theoretically favorable region can be explored in the near future colliders.

## 4 Phenomenology of TeV Scale $B - L$ Model

Based on the simple assumption of classical conformal invariance, we have proposed a minimal phenomenologically viable model with an extra gauge symmetry. The naturalness of the SM Higgs boson mass constrains the  $B - L$  breaking scale to be around TeV and hence, the mass scale of new particles in the model,  $Z'$  boson, right-handed Majorana neutrinos and the SM singlet Higgs boson, is around TeV or smaller. These new particles may be discovered at future collider experiments such as the LHC and ILC. Now we study phenomenology of these new particles.

### 4.1 Search for the $Z'$ boson

We first investigate the  $Z'$  boson production at the LHC. In our study, we calculate the dilepton production cross sections through the  $Z'$  boson exchange together with the SM processes mediated by the  $Z$  boson and photon<sup>2</sup>. The dependence of the cross section on the final state dilepton invariant mass  $M_{ll}$  is described as

$$\begin{aligned} \frac{d\sigma(pp \rightarrow \ell^+\ell^- X)}{dM_{ll}} &= \sum_{a,b} \int_{-1}^1 d\cos\theta \int_{\frac{M_{ll}^2}{E_{\text{CMS}}^2}}^1 dx_1 \frac{2M_{ll}}{x_1 E_{\text{CMS}}^2} \\ &\times f_a(x_1, Q^2) f_b\left(\frac{M_{ll}^2}{x_1 E_{\text{CMS}}^2}, Q^2\right) \frac{d\sigma(\bar{q}q \rightarrow \ell^+\ell^-)}{d\cos\theta}, \end{aligned} \quad (20)$$

where  $E_{\text{CMS}} = 14$  TeV is the center-of-mass energy of the LHC. In our numerical analysis, we employ CTEQ5M [21] for the parton distribution functions with the factorization scale  $Q = m_{Z'}$ . Formulas to calculate  $d\sigma(\bar{q}q \rightarrow \ell^+\ell^-)/d\cos\theta$  are listed in Appendix.

Fig. 6 shows the differential cross section for  $pp \rightarrow \mu^+\mu^-$  for  $m_{Z'} = 2.5$  TeV together with the SM cross section mediated by the  $Z$ -boson and photon. Here, we have used  $\alpha_{B-L} = 0.008$  and all three right-handed Majorana neutrino masses have been fixed to be 200 GeV as an example. The result shows a clear peak of the  $Z'$  resonance. When we choose a kinematical region for the invariant mass in the range,  $M_{Z'} - 2\Gamma_{Z'} \leq M_{ll} \leq M_{Z'} + 2\Gamma_{Z'}$  with  $\Gamma_{Z'} \simeq 53$  GeV, for example, 560 signal events would be observed with an integrated luminosity of  $100 \text{ fb}^{-1}$ , while only a few events are expected for the SM background. We can conclude that the discovery of the  $Z'$  boson with mass around a few TeV and the  $B - L$  gauge coupling comparable to the SM gauge couplings is promising at the LHC.

In order to evaluate the search reach of the  $Z'$  boson at the LHC, more elaborate study is necessary. We refer recent studies in [22]. In Fig. 5, the dashed line (in blue) shows the  $5\text{-}\sigma$

---

<sup>2</sup> The quark pair production channel, in particular, top-quark pair production via the  $Z'$  boson exchange is also worth investigating [19], since top-quark, which electroweakly decays before hadronization, can be used as an ideal tool to probe new physics beyond the Standard Model [20].

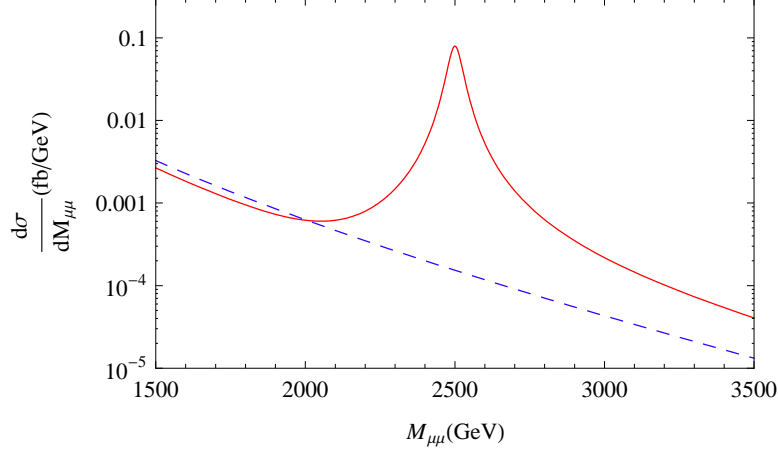


Figure 6: The differential cross section for  $pp \rightarrow \mu^+\mu^-X$  at the LHC for  $m_{Z'} = 2.5$  TeV and  $\alpha_{B-L} = 0.008$ .

discovery limit obtained in [22] for  $E_{\text{CMS}} = 14$  TeV with an integrated luminosity of  $100 \text{ fb}^{-1}$ . If the  $B-L$  gauge coupling is comparable to the SM ones,  $\alpha_{B-L} = \mathcal{O}(0.01)$ , the LHC can cover the region  $m_{Z'} \lesssim 5$  TeV.

Once a resonance of the  $Z'$  boson has been discovered at the LHC, the  $Z'$  boson mass can be determined from the peak energy of the dilepton invariant mass. After the mass measurement, we need more precise measurement of the  $Z'$  boson properties such as couplings with each (chiral) SM fermion, spin and etc., in order to discriminate different models which predict electric-charge neutral gauge bosons. It is interesting to note that the ILC is capable for this task even if its center-of-mass energy is far below the  $Z'$  boson mass [23]. In fact, the search reach of the ILC can be beyond the LHC one.

We calculate the cross sections of the process  $e^+e^- \rightarrow \mu^+\mu^-$  at the ILC with a collider energy  $\sqrt{s} = 1$  TeV for various  $Z'$  boson mass. The deviation of the cross section in our model from the SM one,

$$\frac{\sigma(e^+e^- \rightarrow \gamma, Z, Z' \rightarrow \mu^+\mu^-)}{\sigma_{SM}(e^+e^- \rightarrow \gamma, Z \rightarrow \mu^+\mu^-)} - 1, \quad (21)$$

is depicted in Fig. 7 as a function of  $m_{Z'}$ . Here we have fixed  $\alpha_{B-L} = 0.01$  and the differential cross section is integrated over a scattering angle  $-0.95 \leq \cos\theta \leq 0.95$ . Even for a large  $Z'$  boson mass, for example,  $m_{Z'} = 10$  TeV, Fig. 7 shows a few percent deviations, which is large enough for the ILC with an integrated luminosity  $500 \text{ fb}^{-1}$  to identify. Assuming the ILC is accessible to 1 % deviation, the search limit at the ILC has been investigated in [22] and in Fig. 5, the dotted line (in red) shows the result. The ILC search limit is beyond the one at the LHC.

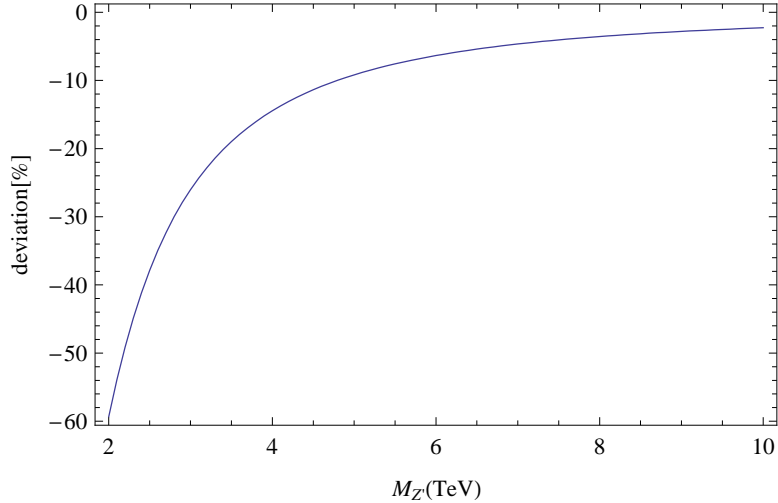


Figure 7: Deviation (in units of %) from the SM cross section as a function of  $M'$ , for  $\alpha_{B-L} = 0.01$ .

The discovery of the  $Z'$  boson has also an impact on neutrino physics. In our model, tiny neutrino masses are obtained by the seesaw mechanism after integrating out the heavy right-handed Majorana neutrinos. As we discussed in the previous section, there is an upper bound on the Yukawa coupling of the right-handed neutrinos not to destabilize the  $B - L$  symmetry breaking minimum,  $\alpha_N < 9.8\alpha_{B-L}$ . Thus, it is likely that right-handed neutrinos are light enough to be produced by  $Z'$  boson decay. If this is the case, the way to investigate the seesaw mechanism is opened up. Once the  $Z'$  boson is produced, it decays into a right-handed neutrino with a branching ratio  $\text{Br}(Z' \rightarrow \nu_R^i \nu_R^i) \simeq 6\%$  (see Appendix for partial decay widths of the  $Z'$  boson). Produced right-handed neutrinos decay into the SM Higgs boson and the weak gauge bosons through the mixing with the SM left-handed neutrinos and provide a signature at the LHC through trilepton final states with a small SM background [24] and events of like-sign leptons associated with the Majorana nature of the right-handed neutrinos [25].

The leptogenesis [26] through the lepton number and CP violating decays of the right-handed Majorana neutrino is a very simple mechanism for baryogenesis, the origin of the baryon asymmetry in the universe. In normal thermal leptogenesis scenario, there is a lower mass bound on the lightest right-handed neutrino,  $m_N \gtrsim 10^9$  GeV [27], in order to achieve the realistic baryon asymmetry in the present universe. In our model, the right-handed neutrino mass is around TeV scale or smaller and far below this bound. In this case, the leptogenesis can be possible through the resonant leptogenesis mechanism [28] due to an enhancement of the CP asymmetry parameter  $\epsilon$  via well-degenerated right-handed neutrinos. If the CP asymmetry parameter is sufficiently large by the resonant leptogenesis mechanism, the difference between



the number of positive and negative like-sign dileptons from the right-handed neutrino decays can be detectable at the LHC [29].

## 4.2 Phenomenology of the SM singlet Higgs boson

Let us finally consider another new particle in the present model, the SM singlet Higgs boson  $\phi$ , and its phenomenological implications. According to the analysis in the previous section, the singlet Higgs boson is relatively light to the  $Z'$  boson, for example, an order of magnitude lighter for  $\alpha_{B-L} \sim 0.01$ . This fact is a general consequence from radiative symmetry breaking by the CW mechanism. This light SM singlet Higgs can be mixed up with the SM Higgs boson through the third term in Eq. (4) and thus, it potentially affects phenomenology of Higgs boson [30].

In our model, because of the absence of tree-level mass terms under the classical conformal invariance, the mixing angle between the SM Higgs and singlet Higgs bosons is not an independent parameter. Using the relation  $\lambda' = -m_h^2/M^2$ , the scalar mass matrix is given by

$$\mathcal{M} = \begin{pmatrix} m_h^2 & -m_h^2 \left(\frac{v}{M}\right) \\ -m_h^2 \left(\frac{v}{M}\right) & m_\phi^2 \end{pmatrix}, \quad (22)$$

where  $m_\phi^2 = 96\alpha_{B-L}^2 M^2$  by neglecting  $\alpha_N^i$ , for simplicity. The mixing angle is described as

$$\tan 2\theta = \frac{2m_h^2(v/M)}{m_h^2 - 96\alpha_{B-L}^2 M^2}. \quad (23)$$

For  $m_h^2 \gtrsim m_\phi^2$ ,  $\tan 2\theta \sim 2v/M \lesssim 0.1$ , while  $\tan 2\theta \sim -2(m_h/m_\phi)^2(v/M) \ll 1$  for  $m_h^2 \ll m_\phi^2$ . In both cases, the mixing angle is small.

In models with multiple SM singlet Higgs scalars, the restrictions on the parameter space from precision electroweak measurements have been investigated [31]. Contributions of the SM singlet Higgs boson to the  $S$ ,  $T$  and  $U$  parameters are roughly proportional to the mixing angle squared [32] and hence negligible in our case. We have checked that the range of SM Higgs boson mass favored by the electroweak precision measurements is shifted, at most, by a few GeV in our model.

If the singlet Higgs boson is light enough, the SM Higgs boson can decay into a pair of the singlets. This partial decay width is found to be

$$\Gamma(h \rightarrow \phi\phi) = \frac{1}{32\pi} \frac{v^2 m_h^3}{M^4} \sim 1.6 \times 10^{-5} \text{ GeV} \quad (24)$$

for  $m_h = 130$  GeV and  $M = 3$  TeV, for example. We compare this width to the partial decay width into bottom quarks,

$$\Gamma(h \rightarrow b\bar{b}) = \frac{3}{8\pi} \frac{m_b^2}{v^2} m_h \sim 2.3 \times 10^{-3} \text{ GeV}, \quad (25)$$

which is the dominant decay mode for  $m_h = 130$  GeV. The branching fraction into a pair of the singlet Higgs bosons is small,  $\text{Br}(h \rightarrow \phi\phi) = \mathcal{O}(0.01)$ . Once the singlet Higgs bosons are produced, they mainly decay into bottom quarks through the mixing with the SM Higgs boson. Note that this process, Higgs boson production and its decay into a pair of the singlet Higgs boson followed by their decays into bottom quarks, is similar to the Higgs boson pair production through the Higgs self-coupling. Here, let us consider Higgs pair production associated with  $Z$  boson,  $e^+e^- \rightarrow Z^* \rightarrow Zh^* \rightarrow Zhh$ , at the ILC [33]. The production cross section is of order 0.1 fb for a collider energy 500 GeV-1 TeV. On the other hand, the pair of the singlet Higgs bosons are produced via  $e^+e^- \rightarrow Z^* \rightarrow Zh$ , followed by the SM Higgs decay  $h \rightarrow \phi\phi$ . In fact, this production cross section is comparable to the one for the Higgs pair production,  $\sigma = \sigma(e^+e^- \rightarrow Zh) \times \text{Br}(h \rightarrow \phi\phi) \sim \mathcal{O}(10\text{fb}) \times 0.01 \sim 0.1$  fb. Experiments for precision measurements of the Higgs self-coupling may reveal the light singlet Higgs boson.

Once the  $Z'$  boson is discovered, the best way to search for the singlet Higgs boson would be its production associated with  $Z'$  boson, which is analogous to the SM Higgs boson search at LEP2, for example. If a future collider such as the ILC has its energy high enough to produce  $Z'$  boson and the singlet Higgs boson, it would be easy to discover the singlet Higgs boson.

## 5 Conclusions

In this paper we have investigated the minimal  $B - L$  model as a phenomenologically viable model in which the Coleman-Weinberg mechanism of the electroweak symmetry breaking does work. Because of the theoretical requirements of the classical conformal invariance, stability of the potential up to the Planck scale and the naturalness of the electroweak scale against the  $B - L$  sector, the parameter region of the model is strongly constrained. We are thus led to the minimal  $B - L$  model naturally realized at the TeV scale. This is a remarkable finding because in the usual minimal  $B - L$  model, there is no special reason for the  $B - L$  symmetry breaking scale to be around the TeV scale and the breaking scale can be much higher without any theoretical and experimental problems.

According to the TeV scale  $B - L$  symmetry breaking, all new particles introduced in addition to the SM particles have masses around the TeV scale or even smaller, so that some signatures of such particles can be expected at future experiments. In particular, the  $Z'$  boson with a few TeV mass is promising to be discovered at the LHC when the  $B - L$  gauge coupling is not too small, say,  $\alpha_{B-L} \gtrsim 0.005$ . Once the  $Z'$  boson is discovered, it will be a portal to explore the  $B - L$  sector. In our model, it is very likely that the right-handed neutrinos are sufficiently light so that it can be pair-produced by the  $Z'$  boson decay. Through the  $Z'$  boson production, the seesaw mechanism can be investigated at the future colliders.

A general consequence of the CW symmetry breaking is a prediction of a relatively light SM singlet Higgs boson compared to the  $Z'$  gauge boson. We have shown that the SM singlet Higgs boson can be as light as the SM Higgs boson. Although this light singlet Higgs boson can mix with the SM Higgs boson and potentially affects on Higgs phenomenology, the effects are found to be small because of a small mixing angle according to the absence of the tree-level mass terms in the scalar potential. Precision measurements of the Higgs self-couplings may reveal the existence of the SM singlet Higgs boson. Again, once the  $Z'$  boson is discovered, the  $Z'$  boson can be used to discover the light singlet Higgs boson. For example, if the energy of the ILC is high enough,  $\sqrt{s} > m_{Z'} + m_\phi$ , the singlet Higgs boson can be produced through the process,  $e^+e^- \rightarrow Z'^* \rightarrow Z'\phi$ , which is completely analogous to the process at LEP2 experiment to search for the SM Higgs boson. In order to confirm the CW symmetry breaking, it is crucial to check the mass relation in Eq. (13).

# Appendix

## A Calculation of the two-loop diagrams

In this appendix we calculate the two loop diagrams in Fig. 4. In order to evaluate them, we first calculate the 2-loop vacuum diagram of Fig. 8, and then take terms proportional to  $m_{Z'}^2 m_t^2$  by taking the second derivatives with respect to  $m_{Z'}$  and  $m_t$ .

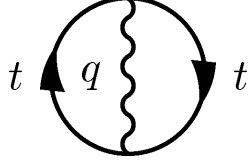


Figure 8: 2-loop vacuum diagram of a top-quark and a  $Z'$  gauge boson with momentum  $q$ .

The 2-loop vacuum diagram can be easily calculated as

$$\int \frac{d^d q}{(2\pi)^d} i\Pi_2(q^2) (q^2 g^{\mu\nu} - q^\mu q^\nu) \frac{-ig^{\mu\nu}}{q^2 - m_{Z'}^2} \quad (26)$$

in terms of the top-quark contribution to the 1-loop self-energy diagram of the  $Z'$  boson

$$\Pi^{\mu\nu}(q) = i (q^2 g^{\mu\nu} - q^\mu q^\nu) \Pi_2(q^2), \quad (27)$$

where  $\Pi_2(q^2)$  is given by

$$\Pi_2(q^2) = -\frac{8g_{B-L}^2}{3(4\pi)^{\frac{d}{2}}} \int_0^1 dx x(1-x) \frac{\Gamma(2 - \frac{d}{2})}{(m_t^2 - x(1-x)q^2)^{2 - \frac{d}{2}}}. \quad (28)$$

Then by taking derivatives we can obtain the terms proportional to  $m_{Z'}^2 m_t^2$  as

$$\begin{aligned} & \frac{\partial^2}{\partial m_t^2 \partial m_{Z'}^2} \int \frac{d^d q}{(2\pi)^d} i\Pi_2(q^2) (q^2 g^{\mu\nu} - q^\mu q^\nu) \frac{-ig^{\mu\nu}}{q^2 - m_{Z'}^2} \\ &= -\frac{8ig_{B-L}^2 \Gamma(3 - \frac{d}{2})}{3(4\pi)^{\frac{d}{2}}} \int \frac{d^d q}{(2\pi)^d} \frac{d-1}{q^4} \sim -\frac{8ig_{B-L}^2}{(4\pi)^4} \log \frac{M_{Pl}^2}{m_{Z'}^2}. \end{aligned} \quad (29)$$

## B Helicity amplitudes

Here we provide formulas useful for calculations of cross sections discussed in this paper. We begin with the following interaction between a massive gauge boson ( $A_\mu$ ) with mass  $m_A$  and a pair of the SM fermions,

$$\mathcal{L}_{\text{int}} = J^\mu A_\mu = \bar{\psi}_f \gamma^\mu (g_L^f P_L + g_R^f P_R) \psi_f A_\mu. \quad (30)$$

A helicity amplitude for the process  $f(\alpha)\bar{f}(\beta) \rightarrow F(\delta)\bar{F}(\gamma)$  is given by

$$\mathcal{M}(\alpha, \beta; \gamma, \delta) = \frac{g_{\mu\nu}}{s - m_A^2 + im_A\Gamma_A} J_{\text{in}}^\mu(\alpha, \beta) J_{\text{out}}^\nu(\gamma, \delta), \quad (31)$$

where  $\alpha, \beta$  ( $\gamma, \delta$ ) denote initial (final) spin states for fermion and anti-fermion, respectively, and  $\Gamma_A$  is the total decay width of the  $A$  boson. We have used 't Hooft-Feynman gauge for the gauge boson propagator and there is no contribution from Nambu-Goldstone modes in the process with the massless initial states.

The currents for initial (massless) and final (massive) states are explicitly given by

$$J_{\text{in}}^\mu(+, -) = -\sqrt{s}g_R^f(0, 1, i, 0), \quad J_{\text{in}}^\mu(-, +) = -\sqrt{s}g_L^f(0, 1, -i, 0), \quad (32)$$

and

$$\begin{aligned} J_{\text{out}}^\mu(+, +) &= \omega_+\omega_- [g_L^F(1, -\sin\theta, 0, -\cos\theta) - g_R^F(1, \sin\theta, 0, \cos\theta)], \\ J_{\text{out}}^\mu(-, -) &= \omega_+\omega_- [g_L^F(1, \sin\theta, 0, \cos\theta) - g_R^F(1, -\sin\theta, 0, -\cos\theta)], \\ J_{\text{out}}^\mu(+, -) &= \omega_-^2 g_L^F(0, -\cos\theta, i, \sin\theta) - \omega_+^2 g_R^F(0, \cos\theta, -i, -\sin\theta), \\ J_{\text{out}}^\mu(-, +) &= \omega_+^2 g_L^F(0, -\cos\theta, -i, \sin\theta) - \omega_-^2 g_R^F(0, \cos\theta, i, -\sin\theta), \end{aligned} \quad (33)$$

where  $\theta$  is the scattering angle,  $\omega_\pm^2 = \frac{\sqrt{s}}{2}(1 \pm \beta_F)$ ,  $\beta_F = \sqrt{1 - \frac{4m_F^2}{s}}$ , and  $f(F)$  denotes a flavor of initial (final) state of fermions.

The couplings for the SM  $Z$  boson are as follows:

$$\begin{aligned} g_L^\nu &= \frac{e}{\cos\theta_W \sin\theta_W} \frac{1}{2}, \quad g_R^\nu = 0, \\ g_L^l &= \frac{e}{\cos\theta_W \sin\theta_W} \left( -\frac{1}{2} - \sin^2\theta_W(-1) \right), \quad g_R^l = -e(-1) \tan\theta_W, \\ g_L^u &= \frac{e}{\cos\theta_W \sin\theta_W} \left( \frac{1}{2} - \sin^2\theta_W \frac{2}{3} \right), \quad g_R^u = -e \frac{2}{3} \tan\theta_W, \\ g_L^d &= \frac{e}{\cos\theta_W \sin\theta_W} \left( -\frac{1}{2} - \sin^2\theta_W \left( -\frac{1}{3} \right) \right), \quad g_R^d = -e \left( -\frac{1}{3} \right) \tan\theta_W, \end{aligned} \quad (34)$$

where  $\theta_W$  is the weak mixing angle. The couplings for the  $Z'$  boson are much simpler:

$$\begin{aligned} g_L^\nu &= g_R^\nu = g_L^l = g_R^l = -1, \\ g_L^u &= g_R^u = g_L^d = g_R^d = \frac{1}{3}. \end{aligned} \quad (35)$$

## C Decay width

Explicit formulas of the partial decay widths of  $Z'$  boson are the following:

$$\begin{aligned}
\Gamma(Z' \rightarrow \nu_l^i \bar{\nu}_l^i) &= \frac{m_{Z'}}{24\pi}, \\
\Gamma(Z' \rightarrow \nu_h^i \bar{\nu}_h^i) &= \frac{m_{Z'}}{24\pi} \left(1 - \frac{m_N^{i2}}{m_{Z'}^2}\right) \sqrt{1 - 4 \frac{m_N^{i2}}{m_{Z'}^2}}, \\
\Gamma(Z' \rightarrow e^+ e^- / \mu^+ \mu^- / \tau^+ \tau^-) &= \frac{m_{Z'}}{12\pi}, \\
\Gamma(Z' \rightarrow u\bar{u} / c\bar{c}) &= \Gamma(Z' \rightarrow d\bar{d} / s\bar{s} / b\bar{b}) = \frac{m_{Z'}}{36\pi}, \\
\Gamma(Z' \rightarrow t\bar{t}) &= \frac{m_{Z'}}{36\pi} \left(1 - 2 \frac{m_t^2}{m_{Z'}^2}\right) \sqrt{1 - 4 \frac{m_t^2}{m_{Z'}^2}}, \tag{36}
\end{aligned}$$

where  $i = 1, 2, 3$  is the generation index, and  $\nu_l$  ( $\nu_h$ ) denotes the light (heavy) Majorana neutrino mass eigenstate after the seesaw mechanism.

## Acknowledgments

We would like to thank Toru Goto for useful discussions on the 2-loop calculations. The work of N.O. is supported in part by the Grant-in-Aid for Scientific Research from the Ministry of Education, Science and Culture of Japan, No. 18740170.

## References

- [1] S. Iso, N. Okada and Y. Orikasa, Phys. Lett. B **676**, 81 (2009) [arXiv:0902.4050 [hep-ph]].
- [2] W. A. Bardeen, FERMILAB-CONF-95-391-T
- [3] K. A. Meissner and H. Nicolai, arXiv:0907.3298 [hep-th].
- [4] S. R. Coleman and E. J. Weinberg, Phys. Rev. D **7**, 1888 (1973).
- [5] K. A. Meissner and H. Nicolai, Phys. Lett. B **648**, 312 (2007) [arXiv:hep-th/0612165]; Phys. Lett. B **660**, 260 (2008) [arXiv:0710.2840 [hep-th]]; Eur. Phys. J. C **57**, 493 (2008) [arXiv:0803.2814 [hep-th]].
- [6] A. G. Dias, Phys. Rev. D **73**, 096002 (2006) [arXiv:hep-ph/0604219].
- [7] R. Hempfling, Phys. Lett. B **379**, 153 (1996) [arXiv:hep-ph/9604278].

- [8] W. F. Chang, J. N. Ng and J. M. S. Wu, Phys. Rev. D **75**, 115016 (2007) [arXiv:hep-ph/0701254].
- [9] R. Foot, A. Kobakhidze and R. R. Volkas, Phys. Lett. B **655**, 156 (2007) [arXiv:0704.1165 [hep-ph]]; Phys. Rev. D **76**, 075014 (2007) [arXiv:0706.1829 [hep-ph]]; Phys. Rev. D **77**, 035006 (2008) [arXiv:0709.2750 [hep-ph]].
- [10] R. N. Mohapatra and R. E. Marshak, Phys. Rev. Lett. **44**, 1316 (1980); R. E. Marshak and R. N. Mohapatra, Phys. Lett. B **91**, 222 (1980); C. Wetterich, Nucl. Phys. B **187**, 343 (1981); A. Masiero, J. F. Nieves and T. Yanagida, Phys. Lett. B **116**, 11 (1982); R. N. Mohapatra and G. Senjanovic, Phys. Rev. D **27**, 254 (1983); W. Buchmuller, C. Greub and P. Minkowski, Phys. Lett. B **267**, 395 (1991).
- [11] S. Khalil, J. Phys. G **35**, 055001 (2008) [arXiv:hep-ph/0611205].
- [12] E. Gildener and S. Weinberg, Phys. Rev. D **13**, 3333 (1976).
- [13] For a review, see M. Sher, Phys. Rept. **179**, 273 (1989), and references therein.
- [14] K. A. Meissner and H. Nicolai, arXiv:0809.1338 [hep-th].
- [15] U. Ellwanger, Phys. Lett. B **303** (1993) 271; U. Ellwanger, M. Rausch de Traubenberg and C. A. Savoy, Phys. Lett. B **315** (1993) 331; T. Elliott, S. F. King and P. L. White, Phys. Lett. B **351** (1995) 213; S. F. King and P. L. White, Phys. Rev. D **52** (1995) 4183; G. K. Yeghian, arXiv:hep-ph/9904488; U. Ellwanger and C. Hugonie, Mod. Phys. Lett. A **22**, 1581 (2007).
- [16] J. A. Casas, J. R. Espinosa and I. Hidalgo, JHEP **0411**, 057 (2004) [arXiv:hep-ph/0410298].
- [17] M. S. Carena, A. Daleo, B. A. Dobrescu and T. M. P. Tait, Phys. Rev. D **70**, 093009 (2004) [arXiv:hep-ph/0408098].
- [18] A. Abulencia *et al.* [CDF Collaboration], Phys. Rev. Lett. **96**, 211801 (2006) [arXiv:hep-ex/0602045].
- [19] See, for example, M. Arai, N. Okada, K. Smolek and V. Simak, Phys. Rev. D **70**, 115015 (2004) [arXiv:hep-ph/0409273]; Phys. Rev. D **75**, 095008 (2007) [arXiv:hep-ph/0701155]; Acta Phys. Polon. B **40**, 93 (2009) [arXiv:0804.3740 [hep-ph]], references therein.
- [20] C. T. Hill and S. J. Parke, Phys. Rev. D **49**, 4454 (1994).

- [21] J. Pumplin, D. R. Stump, J. Huston, H. L. Lai, P. Nadolsky and W. K. Tung, JHEP **07** (2002) 012.
- [22] L. Basso, A. Belyaev, S. Moretti and G. M. Pruna, arXiv:0903.4777 [hep-ph].
- [23] M. Cvetič and S. Godfrey, arXiv:hep-ph/9504216. T. G. Rizzo, arXiv:hep-ph/9612440; S. Godfrey, arXiv:hep-ph/0201092; arXiv:hep-ph/0201093.
- [24] J. A. Aguilar-Saavedra, arXiv:0905.2221 [hep-ph].
- [25] K. Huitu, S. Khalil, H. Okada and S. K. Rai, Phys. Rev. Lett. **101**, 181802 (2008) [arXiv:0803.2799 [hep-ph]]; L. Basso, A. Belyaev, S. Moretti and C. H. Shepherd-Themistocleous, arXiv:0812.4313 [hep-ph]; P. F. Perez, T. Han and T. Li, arXiv:0907.4186 [hep-ph].
- [26] M. Fukugita and T. Yanagida, Phys. Lett. B **174**, 45 (1986).
- [27] W. Buchmüller, P. Di Bari and M. Plumacher, Nucl. Phys. B **643**, 367 (2002) [Erratum-ibid. B **793**, 362 (2008)] [arXiv:hep-ph/0205349].
- [28] M. Flanz, E. A. Paschos, U. Sarkar and J. Weiss, Phys. Lett. B **389**, 693 (1996) [arXiv:hep-ph/9607310]; A. Pilaftsis, Phys. Rev. D **56**, 5431 (1997) [arXiv:hep-ph/9707235]; A. Pilaftsis and T. E. J. Underwood, Nucl. Phys. B **692**, 303 (2004) [arXiv:hep-ph/0309342].
- [29] S. Blanchet, Z. Chacko, S. S. Granor and R. N. Mohapatra, arXiv:0904.2174 [hep-ph].
- [30] W. Emam and S. Khalil, Eur. Phys. J. C **522**, 625 (2007) [arXiv:0704.1395 [hep-ph]].
- [31] For a recent paper, see, for example, S. Dawson and W. Yan, arXiv:0904.2005 [hep-ph], references therein.
- [32] M. E. Peskin, T. Takeuchi, Phys. Rev. Lett. **64**, 964 (1990) M. E. Peskin, T. Takeuchi Phys. Rev. D **46**, 381 (1992)
- [33] See, for example, Y. Takubo, arXiv:0907.0524 [hep-ph].